Research Square

Preprints are preliminary reports that have not undergone peer review.
They should not be considered conclusive, used to inform clinical practice,
or referenced by the media as validated information.

Exploration of Diagnostic Biomarkers in Seminal Plasma and Metabolic Mechanisms of Non-Obstructive Azoospermia Based on Metabolomics and Transcriptomics

Wei Wang
Second Hospital of Shanxi Medical University
Pengbo Hua
Second Hospital of Shanxi Medical University
Jinshan Chen
The First Hospital of China Medical University
Chunfeng Li
First Hospital of Shanxi Medical University
Yuan Ji
Second Hospital of Shanxi Medical University
Yujia Xi
Second Hospital of Shanxi Medical University
Shuang Wang
Shanxi Bethune Hospital
Rui Tu
First Hospital of Shanxi Medical University
Yulong Luo
First Hospital of Shanxi Medical University
Binbin Hu
Taiyuan Central Hospital
Yang Zhao
Linfen People's Hospital
Qiang Guo
Second Hospital of Shanxi Medical University
Jingqi Wang
drwangjq@126.com

Second Hospital of Shanxi Medical University

Research Article

Keywords: non-obstructive azoospermia, seminal plasma, metabolomics, transcriptomics, biomarkers, male infertility

Posted Date: November 13th, 2026

DOI: https://doi.org/10.21203/rs.3.rs-11401977/v1

License: This work is licensed under a Creative Commons Attribution 4.0 International License. Read Full License

Additional Declarations: No competing interests reported.

Exploration of Diagnostic Biomarkers in Seminal Plasma and Metabolic Mechanisms of Non-Obstructive Azoospermia Based on Metabolomics and Transcriptomics

Wei Wang[1,2,†], Pengbo Hua[1,2,†], Jinshan Chen[3,†], Chunfeng Li[4], Yuan Ji[1,2], Yujia Xi[1,2], Shuang Wang[5], Rui Tu[4], Yulong Luo[4,] Binbin Hu[6], Yang Zhao[7], Qiang Guo[1,2], Jingqi Wang[1,2]

1 Department of Urology, Second Hospital of Shanxi Medical University, Taiyuan 030000, China

2 Male Reproductive Health Research Center, Shanxi Medical University, Jinzhong 030600, China

3 Department of Vascular Surgery, The First Hospital of China Medical University, Shenyang 110001, China

4 Department of Urology, First Hospital of Shanxi Medical University, Taiyuan 030000, China

5 Department of Gastroenterology, Shanxi Bethune Hospital, Taiyuan 030032, China

6 Department of Reproductive Medicine, Taiyuan Central Hospital, Taiyuan 030000, China

7 Department of Andrology, Linfen People's Hospital, Linfen 041000, China

† These authors contributed equally to this work.

Corresponding author: Jingqi Wang, Department of Urology, Second Hospital of Shanxi Medical University, Taiyuan 030000, China. Email: drwangjq@126.com

Co-corresponding author: Qiang Guo, Department of Urology, Second Hospital of Shanxi Medical University, Taiyuan 030000, China. Email: llgqiang@163.com

Running title: Seminal plasma biomarkers for NOA

Abstract

Background: Non-obstructive azoospermia (NOA) is a severe form of male infertility for which diagnosis may involve invasive testicular biopsy. This study aimed to identify candidate non-invasive biomarkers in seminal plasma and explore metabolic pathways associated with NOA.

Methods: We conducted a cross-sectional study of seminal plasma from 20 men with NOA and 20 normospermic controls recruited at the Second Hospital of Shanxi Medical University between December 2022 and November 2023. Targeted liquid chromatography–mass spectrometry quantified 414 metabolites. Differential metabolites were identified using orthogonal partial least-squares discriminant analysis (variable importance in projection > 1) and t tests ($P < 0.05$), and their diagnostic performance was assessed by receiver operating characteristic analysis. Pathway enrichment was integrated with publicly available testicular transcriptomic data (GSE4797; 16 NOA and 12 control samples).

Results: The NOA and control groups separated in orthogonal partial least-squares discriminant analysis ($Q^2 = 0.72$; $R^2Y = 0.887$; both $P < 0.05$). Seventy-three metabolites met the differential-abundance criteria (variable importance in projection > 1 and $P < 0.05$), including 42 with higher and 31 with lower abundance in NOA. Five metabolites had reported receiver-operating-characteristic areas under the curve of 0.900 for L-pipecolic acid, 0.998 for phenylpyruvic acid, 0.930 for thymidine, 0.905 for thiamine pyrophosphate, and 0.887 for L-methionine sulfone. Integration with transcriptomic data implicated purine, amino-acid, and energy-metabolism pathways and suggested an association with oxidative-

stress-related metabolic dysregulation.

Conclusions: The findings identify candidate seminal-plasma biomarkers and metabolic pathways associated with NOA. The biomarkers require evaluation in larger, independent and multicenter cohorts, including comparison with obstructive azoospermia, before clinical use.

Keywords: non-obstructive azoospermia; seminal plasma; metabolomics; transcriptomics; biomarkers; male infertility

Background

NOA is defined as normal semen volume in patients with no sperm detected in semen analysis after centrifugation on at least two consecutive occasions, with the symptoms of obstructive azoospermia excluded. Typically, it is diagnosed through testicular histopathological biopsy and can be classified into Sertoli cell-only syndrome, spermatogenic cell maturation arrest, and testicular germ cell dysfunction based on histopathological phenotypes [1]. Approximately 70% of the causes of NOA remain unknown and are influenced by individual differences compared to OA. In most cases, patients pursue microdissection testicular sperm extraction surgery; however, the success rate stands at a mere 38%-63% [2]. Consequently, NOA has become one of the most intricate and challenging conditions to treat in male infertility. It brings about heightened psychosocial and marital stress while imposing a significant economic burden on healthcare systems due to the dearth of effective treatment modalities. Although current research primarily focuses on somatic cell immaturity, abnormal expression of growth factor signaling, intensified oxidative stress and inflammation response, increased cell apoptosis, and abnormal regulation of the

extracellular matrix, the pathogenesis of NOA remains incompletely understood. Therefore, further comprehensive research and exploration are imperative.

Metabolomics represents a growing methodology in the field of systems biology, supported by progress in sophisticated analytical technologies and computational biology. It is increasingly employed as an integrative tool in clinical and biomedical investigations. Quantifying the metabolome, which offers a real-time chemical representation of a biological system's phenotype, is now commonly used to decipher disease-related pathophysiological pathways and to discover new biomarkers for diagnosing and predicting various pathological conditions.

This study employed integrated metabolomic and transcriptomic analyses of semen from patients with non-obstructive azoospermia (NOA) to identify seminal metabolic alterations relative to normospermic individuals. By leveraging the direct reflection of phenotype provided by metabolomics, we aimed to discover diagnostic biomarkers in seminal plasma. The goal is to develop a non-invasive diagnostic framework for NOA and elucidate its underlying metabolic mechanisms, thereby reducing reliance on invasive diagnostic procedures.

Methods

Study Subjects

A total of 20 patients with non-obstructive azoospermia (NOA) and 20 healthy individuals were recruited from the Second Hospital of Shanxi Medical University between December 1, 2022, and November 30, 2023, based on specific inclusion criteria. The

inclusion criteria were as follows:

NOA patients: Patients aged 18 years or older but younger than 45 years were included based on the definition of NOA in the "European Association of Urology Guidelines on Male Sexual and Reproductive Health: 2022 Update on Male Infertility " This included patients with normal semen volume and at least two consecutive semen analyses showing the absence of sperm after centrifugation, while excluding obstructive azoospermia.

Healthy individuals: Healthy individuals met the criteria outlined in the "WHO Laboratory Manual for the Examination and Processing of Human Semen" (5th edition). This included criteria as below：

- abstinence from sexual activity for 2-7 days before sample collection
- grayish-white appearance of the semen
- semen liquefaction time ≤ 60 minutes
- parameters related to semen quality
- normal forms semen≥4%
- Sperm concentration≥15*10^6/ml
- Total sperm count≥39*10^6
- Sperm motility：PR≥32%、PR+NP≥40%
- Sperm survival rate≥58%

Exclusion Criteria:

- Patients with obstructive azoospermia
- Patients with reproductive tract or urinary tract infections
- Patients with severe organ dysfunction (e.g., heart, liver, or kidney failure)

- Patients with concomitant tumors, hematological disorders, immune system disorders, or mental illnesses
- Patients who received other treatment regimens during semen collection
- Patients who were unavailable for follow-up or unable to provide semen samples

Data Source

After semen collection from the enrolled patients and healthy individuals, the samples were immediately placed in a 4°C refrigerator. The samples were then centrifuged at 3000 rpm for 10 minutes, and the supernatant was transferred to 1.5 mL cryotubes. The cryotubes were labeled, and the samples were flash-frozen in liquid nitrogen for preservation and stored in a -80°C freezer.

Additionally, for transcriptomic analysis, the dataset GSE4797 containing 12 normal human testicular tissue samples and 16 NOA testicular tissue samples was obtained from the Gene Expression Omnibus (GEO) database (https://www.ncbi.nlm.nih.gov/geo/).

Experimental Methods

Extraction and Detection of Metabolites

Samples were thawed on ice, mixed with distilled water and pre-chilled methanol/acetonitrile (1:1) containing internal standards, then vortexed, sonicated in an ice-water bath, and incubated at -40°C. After centrifugation, the supernatant was concentrated by centrifugal evaporation. The dried residue was reconstituted in an acetonitrile/water (6:4) solution, vortexed, centrifuged again, and the final supernatant was collected for LC-MS

analysis. Chromatographic separation was performed using a Waters UPLC system with an Atlantis Premier BEH Z-HILIC column, while detection was carried out on a SCIEX 6500 QTRAP+ mass spectrometer operating in multiple reaction monitoring (MRM) mode.

Orthogonal Partial Least Square Discriminant Analysis (OPLS-DA)

The collected data were imported into SIMCA software (V16.0.2, Sartorius Stedim Data Analytics AB, Umea, Sweden). The data were logarithmically transformed, and UV scaled to ensure appropriate scaling. OPLS-DA modeling was performed on the principal components. The models were validated using 7-fold cross-validation.

Differential Metabolite Screening

Screening differential metabolites is a crucial objective in metabolomics analysis. The contribution of each metabolite to the model was assessed by calculating correlation coefficients, such as Variable Importance in Projection (VIP) scores, based on the OPLS-DA model. Univariate analysis (UVA) methods, including t-tests and analysis of variance (ANOVA), are commonly used for differential metabolite analysis. However, compared to UVA, multivariate statistical methods offer improved insight into the relationships between metabolites and emphasize their promoting or antagonistic roles in biological processes. To avoid model overfitting and false-positive errors, both approaches were employed in this study. Metabolites were considered differentially expressed when their t-test P-value was less than 0.05 and VIP score was greater than 1. Visualization of differential metabolites was achieved through volcano plots and stick plots using the "ggplot2" package in R.

Correlation Analysis of Differential Metabolites

To gain further understanding of the interactions between differential metabolites, this study conducted correlation analysis using the Pearson method. Positive correlation indicates a synergistic interaction between differential metabolites, while negative correlation suggests opposing trends. The results were visualized as correlation heatmaps using the "corrplot" package in R and chord plots using the "ggraph" package.

Cluster Heatmap Analysis

After preprocessing the raw data obtained from targeted metabolomics, the data was normalized in R software. The "pheatmap" package was utilized to perform cluster heatmap analysis on all samples, with sample grouping as the x-axis and differential metabolite expression levels as the y-axis.

Enrichment Analysis of Differential Metabolites

To understand the involvement of metabolic pathways in differential metabolites, a Kyoto Encyclopedia of Genes and Genomes (KEGG) pathway enrichment analysis was conducted in this study. The results were visualized as bubble plots and differential gene abundance score plots using the "ggplot2" package in R. Additionally, the MetaboAnalyst website (https://www.metaboanalyst.ca/) was utilized for the enrichment analysis of differential metabolites. The results were visualized as bubble plots and treemap plots using the "ggplot2" and "treemap" packages in R. Differential genes were also identified using the "limma" package in R. KEGG pathway enrichment analysis and Gene Ontology (GO) enrichment analysis were performed using the "clusterProfiler" package to explore potential

molecular pathways.

ROC Analysis of Differential Metabolites

Receiver Operating Characteristic (ROC) curves were plotted for each differential metabolite using the "pROC" package in R. ROC curves represent the true positive rate (sensitivity) on the y-axis and the false positive rate (1-specificity) on the x-axis. They are used to screen biomarkers with high sensitivity and specificity. In this study, the area under the curve (AUC) was calculated for each metabolite, and the diagnostic performance was evaluated based on the AUC value. An AUC closer to 1 indicates better diagnostic performance, while AUC values within specific ranges suggest different levels of diagnostic accuracy. An AUC > 0.9 indicates high diagnostic accuracy, $0.7 < AUC \leq 0.9$ suggests moderate diagnostic accuracy, $0.5 < AUC \leq 0.7$ suggests low diagnostic accuracy, and an AUC of 0.5 suggests no diagnostic value.

Transcriptomic Analysis of Differential Metabolites

The "IOBR" package includes several metabolic pathway scoring methods. Therefore, we employed the "IOBR" package to score metabolic pathways and conduct differential analysis.

Comparison Analysis of Baseline Data

Between Groups Descriptive statistics (mean ± standard deviation) were computed for normally distributed continuous data, and independent sample t-tests were used to compare the differences between the NOA group and the normal control (NS) group using SPSS 26.0

software.

Results

Comparison of baseline data between NOA and NS groups

Through the collection and analysis of baseline data from patients, significant differences were found in total sperm count, total sperm motility, and forward motility between the two groups. However, there were no statistically significant differences in patient age and BMI (Table 1).

Table 1 Comparison of baseline data between NOA and NS groups

	NS	NOA	*P*
Age（years）	29.100±0.710	29.410±1.397	0.845
BMI（kg/m^2）	23.885±0.672	23.268±0.433	0.437
Total sperm count（×10^6）	67.536±8.371	0	
Total sperm motility（%）	69.395±4.185	0	
Forward motion force（%）	57.095±3.370	0	

Metabolomics analysis

Orthogonal partial least squares discriminant analysis (OPLS-DA)

Using the unsupervised clustering mode of OPLS-DA, it was found that the NOA and NS groups could be significantly separated and formed distinct clusters, with all samples falling within the 95% confidence interval (Figure 1A). To further validate the stability of the model and avoid model overfitting, a permutation test analysis was conducted, revealing Q^2=0.72 ($P<0.05$) and R^2Y=0.887 ($P<0.05$). These results demonstrate that less than 5% of the random models had better predictive and explanatory abilities than the original model, indicating good predictive and explanatory abilities of the original model (Figure 1B,C).

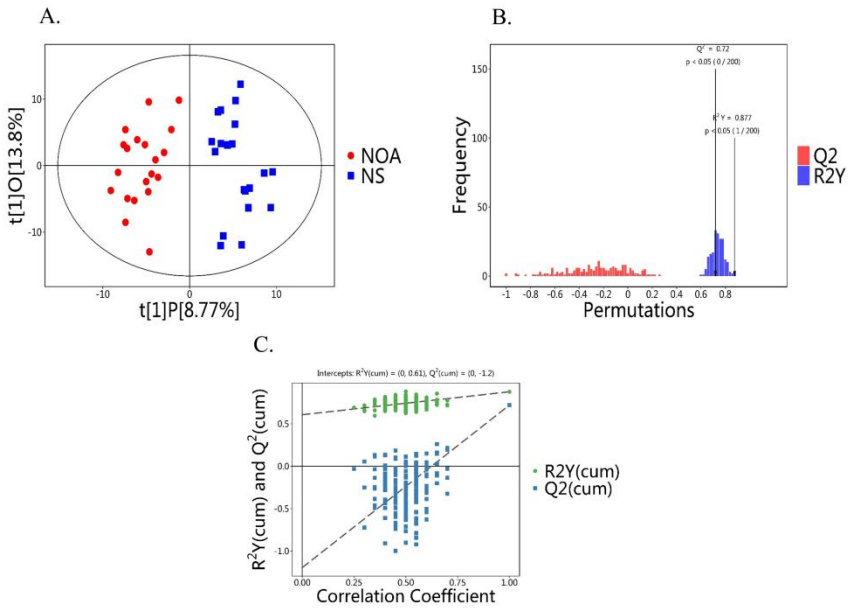


Figure 1. OPLS-DA analysis of targeted metabolomics data. A. Permutation test bar plot for the OPLS-DA model. B. Permutation test for the OPLS-DA model. C. Scatter plot of OPLS-DA model scores.

Differential analysis of metabolites

Targeted quantitative analysis of 414 metabolites was conducted, setting the differential threshold based on VIP>1 and P<0.05. A total of 73 differentially regulated metabolites were identified, with 42 metabolites upregulated and 31 metabolites downregulated in the NOA group compared to the NS group. These differentially regulated metabolites were mainly concentrated in categories such as amino acids, peptides, and their derivatives (Tables 2 and 3). The top 10 upregulated metabolites included mangiferin, isonicotinic acid, nicotinic acid, pyridine-2-carboxylic acid, uracil, glycylphenylalanine, gamma-glutamylvaline, N6-acetyl-L-lysine, l-pipecolic acid, and L-dopa. The top 10 downregulated metabolites included deoxyadenosine, thymidine, butyl betaine, L-methionine sulfoxide, adenosine, acetylcholine, thiamine pyrophosphate, niacinamide, bilirubin, and inosine. In order to observe the differences in metabolites between the two groups more intuitively, volcano plots, cluster

heatmaps, and stick plots were used for detailed visualization (Figure 2 A-C).

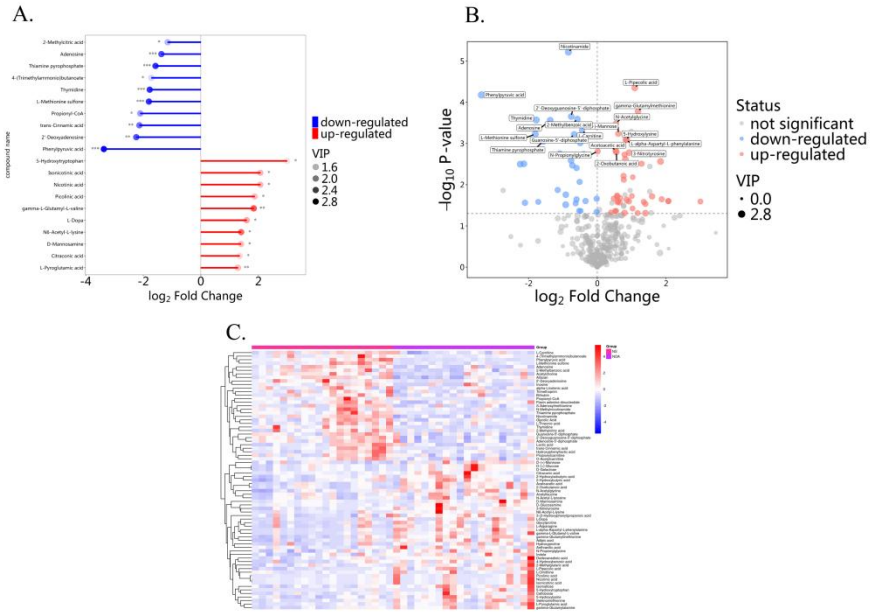


Figure 2 Differential analysis of targeted metabolomics. (A) Volcano plot displaying metabolite fold changes (log2) against statistical significance (-log10 p-value). Point color intensity corresponds to the VIP value from the OPLS-DA model. (B) Scatter plot illustrating the relationship between fold change and p-value from t-tests. The size of the scatter points represents the VIP value. (C) Heatmap showing the relative abundance of differential metabolites across groups. Red and blue colors indicate high and low expression levels, respectively.

Interactions between metabolites

Metabolites are known to interact with each other. After analyzing the interaction of 73 different metabolites, it was found that there is mainly interaction among metabolites of the same category. In addition, significant correlations were observed between adipic acid and N6-acetyl-L-lysine, L-ornithylglycine, L-phenylglycine, and γ-glutamylmethionine (Figure 3).

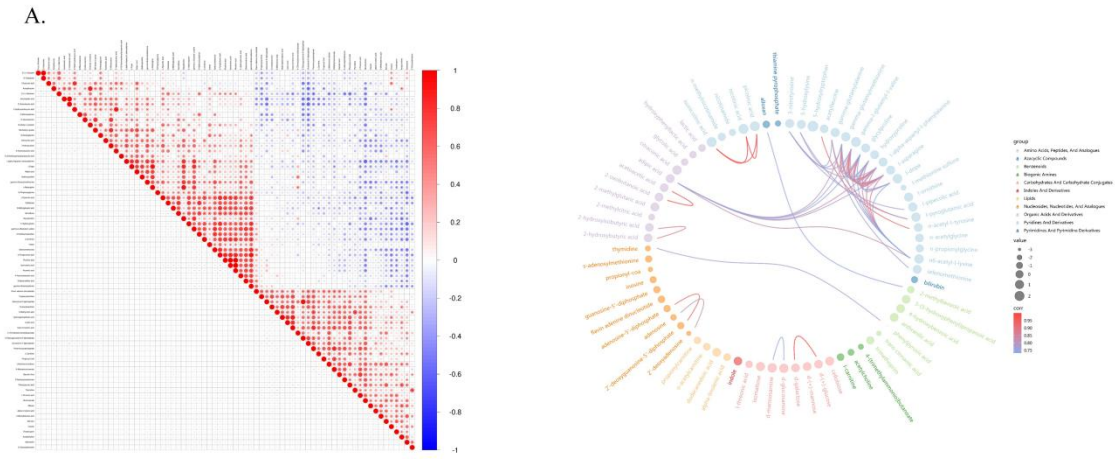


Figure 3. Correlation analysis of differentially expressed metabolites. A. Correlation heatmap showing the correlation coefficient between metabolites at different positions. The color blocks represent the magnitude of correlation, with red indicating positive correlation and blue indicating negative correlation. Darker colors represent stronger correlation. B. Chord diagram of differentially expressed metabolites. The size of the dots represents the magnitude of LOGFC values, with larger dots indicating larger corresponding LOGFC values. The color of the dots represents the classification of differentially expressed metabolites. The lines represent the magnitude of correlation coefficient values between metabolites at corresponding positions.

Metabolic pathway analysis

To elucidate the metabolic mechanisms underlying the condition, KEGG enrichment and metabolic pathway analyses were performed on the differentially expressed metabolites. The results revealed significant involvement in multiple key pathways, including lysine degradation, glycolysis/gluconeogenesis, propanoate metabolism, amino acid biosynthesis, nucleotide and purine metabolism, as well as the cAMP signaling pathway. Notably, metabolites in propanoate metabolism, nucleotide and purine metabolism, and the cAMP signaling pathway showed a marked downregulation trend (Figure 4. Further pathway analysis highlighted several additional processes potentially critical to disease pathogenesis, such as ketone body synthesis and degradation, phenylalanine metabolism, pyrimidine

metabolism, the TCA cycle, starch and sucrose metabolism, glycine/serine/threonine metabolism, cysteine and methionine metabolism, and niacin/nicotinamide metabolism (Figure 5 A, B). These findings suggest a widespread disruption of energy metabolism and amino acid/nucleotide homeostasis in the disease state.

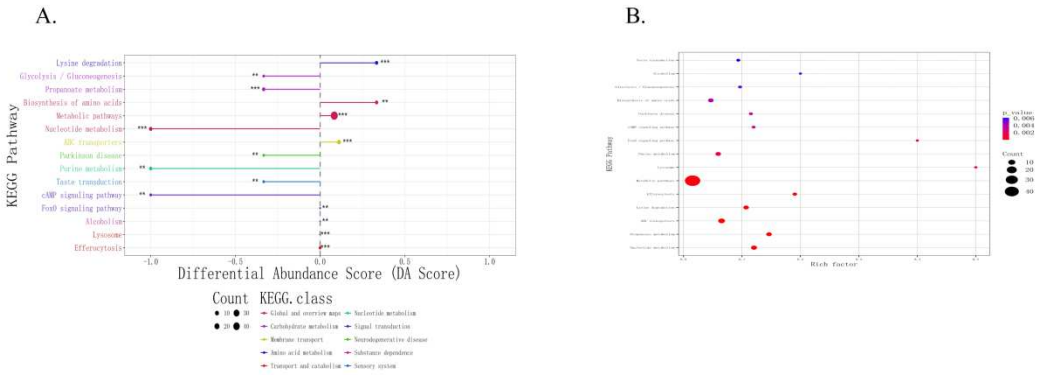


Figure 4. KEGG enrichment of differentially expressed metabolites. A. Differential abundance score plot for KEGG enrichment. B. Enrichment analysis of metabolic pathways for metabolite biomarkers.

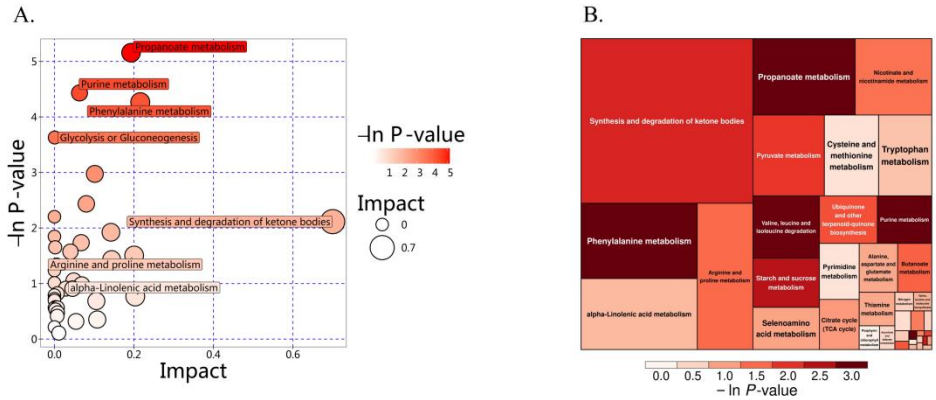


Figure 5. Metabolic pathway analysis of differentially expressed metabolites. A. Pathway analysis bubble plot of

differentially expressed metabolites. The y-axis and bubble color represent the p-values from the enrichment analysis, with darker colors indicating smaller p-values and more significant enrichment. B. Rectangular tree plot of pathway analysis for differentially expressed metabolites.

ROC analysis

ROC analysis was used to evaluate the performance of 73 differentially regulated metabolites in diagnosing NOA. Five metabolites had an AUC value equal to or greater than 0.880. Among the upregulated metabolites, L-Pipecolic acid (AUC=0.900) may serve as a more promising diagnostic marker for NOA (Figure 6A). Among the downregulated metabolites, Phenylpyruvic acid (AUC=0.998), Thymidine (AUC=0.930), Thiamine pyrophosphate (AUC=0.905), and L-Methionine sulfone (AUC=0.887) may represent more favorable diagnostic markers for NOA (Figure 6B).

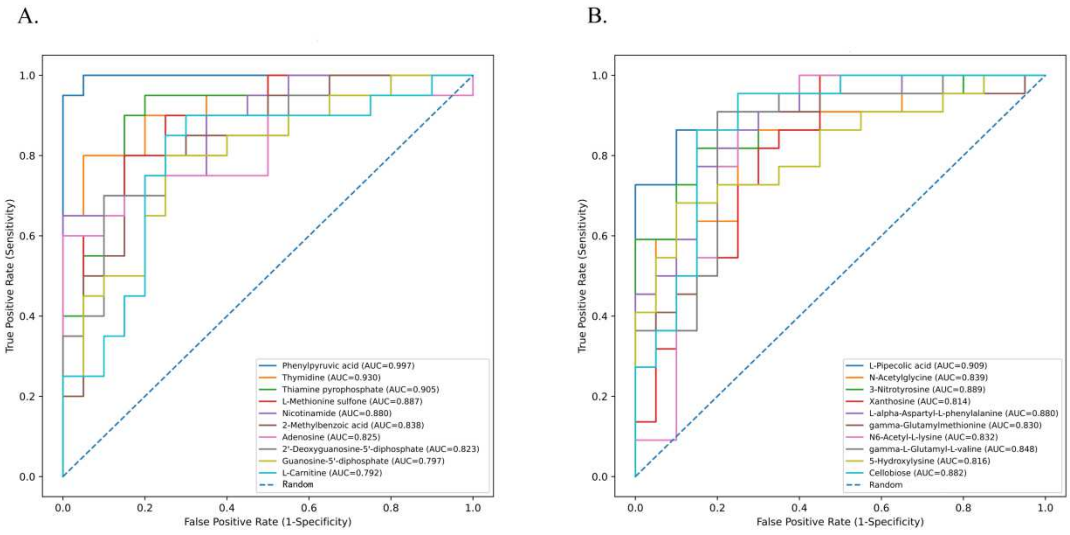


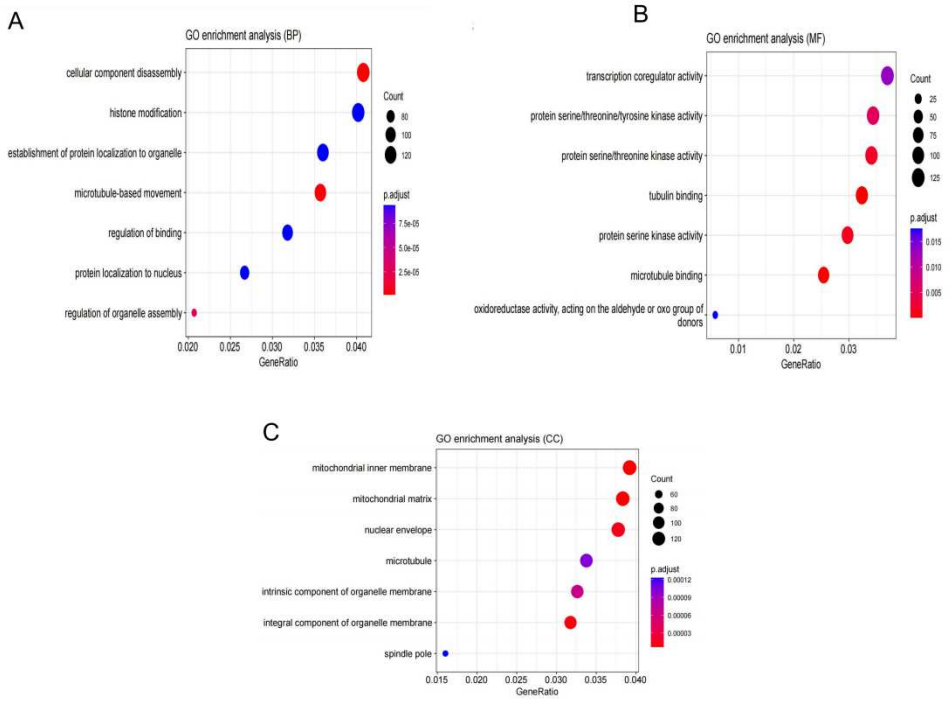
Figure 6. Receiver-operating-characteristic curves for selected differential metabolites. (A) Metabolites higher in NOA. (B) Metabolites lower in NOA. AUC, area under the curve; NOA, non-obstructive azoospermia.

Transcriptomics and integrated metabolomics analysis

Gene Ontology enrichment analysis of GSE4797 identified terms including cellular

component assembly, histone modification, mitochondrial inner membrane, mitochondrial matrix, transcription regulator activity, and threonine/serine/tyrosine kinase activity (Figure 7). Differential analysis identified 2,369 upregulated and 1,307 downregulated genes in NOA relative to controls (Figure 8A). KEGG enrichment identified pathways related to neurodegenerative diseases, autophagy, and purine metabolism (Figure 8B).

Conventional differential gene enrichment analysis often overlooks the impact of subtle gene differences on pathways. In this study, based on the gene expression profiles of GSE4797, enrichment scoring was performed on KEGG pathways to evaluate the pathway differences between the NOA group and the NS group. It was found that there were significant differences in purine metabolism, lysine degradation, and starch and sucrose metabolism pathways (Figure 8 C), which were consistent with the results of metabolomics KEGG enrichment analysis. To expand the comparison of metabolic pathways, differential analysis was conducted on a set of collected metabolic pathway sets. It was observed that there were significant differences in pathways such as purine metabolism, lysine degradation, starch and sucrose metabolism, glycine/serine/threonine metabolism, cysteine and methionine metabolism, niacin and nicotinamide metabolism, and arginine and proline metabolism (Figure 8 D), which were consistent with the results of metabolomics metabolic pathway enrichment analysis.



293

294 Figure 7 Bubble plot of Gene Ontology (GO) enrichment.

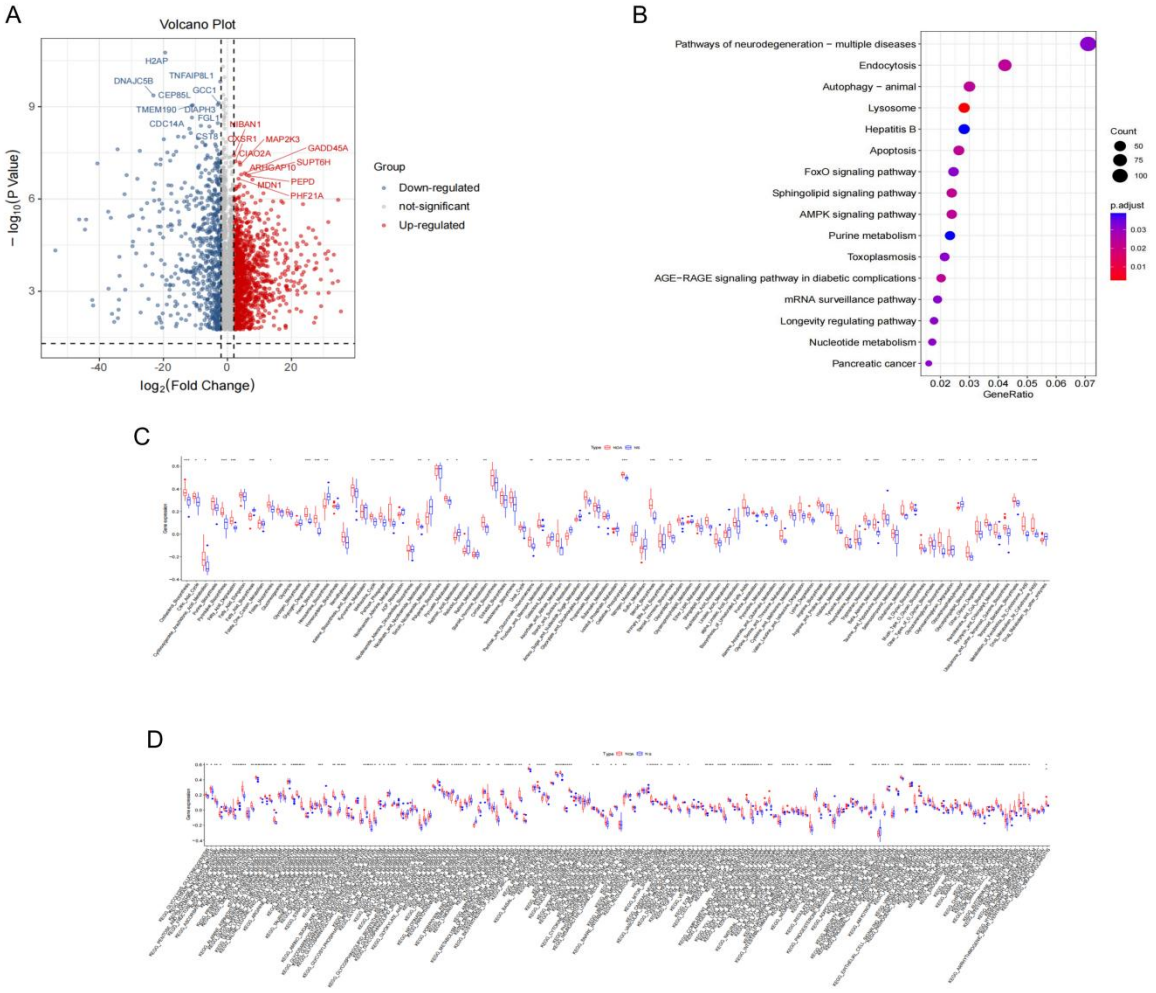


Figure 8. Integration of testicular transcriptomics and seminal-plasma metabolomics. (A) Volcano plot of differentially expressed genes in GSE4797; red indicates higher and blue indicates lower expression in NOA. (B) KEGG pathway enrichment of differentially expressed genes. (C) Boxplots of metabolic pathway scores. (D) Boxplots of KEGG pathway scores. NOA, non-obstructive azoospermia.

Discussion

NOA, a severe form of male infertility characterized by defective spermatogenesis, poses a substantial clinical and societal burden. Current diagnostic methods often rely on invasive procedures, which are undesirable for patients[3]. Recent advances in metabolomics have enabled the identification of biomarkers for male infertility, offering potential non-invasive alternatives. In this study, we performed metabolomic and transcriptomic profiling of

semen samples from NOA patients to explore a novel non-invasive diagnostic approach.

Oxidative stress is a major contributor to male infertility [4], and related seminal biomarkers including reactive oxygen species (ROS; AUC=0.683) [5], total antioxidant capacity (TAC; AUC=0.608) [6], ROS-TAC (AUC=0.845) [7], and oxidation-reduction potential (ORP; AUC=0.648–0.754) [8] have shown diagnostic potential. Fatty acids such as palmitic acid and oleic acid have also been implicated in infertility diagnostics (AUC=0.729–0.862) [9]. However, most previous studies relied on untargeted metabolomics without quantitative analysis of non-obstructive azoospermia (NOA). In this study, targeted metabolomics quantified 414 metabolites, identifying 73 differentially expressed metabolites. Six metabolites—L-Pipecolic acid (AUC=0.900), Phenylpyruvic acid (AUC=0.998), Thymidine (AUC=0.930), Thiamine pyrophosphate (AUC=0.905), L-Methionine sulfone (AUC=0.888), and Nicotinamide (AUC=0.880)—demonstrated high diagnostic accuracy for NOA (AUC $\geq$ 0.880). Except for nicotinamide, which is used in semen preservation, the other five metabolites have not been previously linked to male infertility, suggesting novel candidates for non-invasive NOA diagnosis. Further validation in larger cohorts is warranted to confirm their diagnostic stability and pathological relevance.

Differentially enriched metabolites in the purine metabolism pathway include adenosine diphosphate, adenosine, deoxyadenosine, xanthine, inosine, deoxyguanosine diphosphate, and glycine. Studies have shown that the observed changes in the purine metabolism pathway in infertile males may be associated with decreased sperm quality. Several studies have found that non-metabolized xanthine, through the inhibition of cAMP degradation, may be an important factor causing meiotic arrest in mouse oocytes, providing important clues for the

study of male NOA[10]. Abnormalities in the metabolism of inosine and xanthine may affect sperm vitality and fertilization capacity [11, 12]. Additionally, xanthine, a nucleoside derived from xanthine, is a chemical substance that increases in male seminal plasma after vasectomy, and the disruption of its oxidase system is closely related to energy metabolism and oxidative stress in male infertility [13, 14]. Furthermore, Jie et al. found that abnormal purine metabolism in urine analysis of oligozoospermia patients is also associated with the occurrence of oligozoospermia, providing additional indirect evidence. These findings suggest that disturbances in purine metabolism may be one of the important factors leading to NOA but further exploration is needed.

Regarding amino acid metabolism, the detected alterations in metabolites like S-adenosylmethionine (SAM) and L-methionine are of particular interest. SAM plays a critical role in cellular processes, and its decreased levels have been associated with impairments in sperm concentration and motility [15,16]. The differentially enriched metabolites in the niacin and niacinamide metabolism pathway mainly include niacin and niacinamide. Niacin, also known as vitamin B3, is a water-soluble vitamin that is commonly used to reduce the risk of cardiovascular diseases and improve metabolic syndrome due to its lipid-regulating properties[17]. Niacinamide is an amide compound of niacin and is a precursor of nicotinamide adenine dinucleotide (NAD) and nicotinamide adenine dinucleotide phosphate (NADP). It is associated with the treatment of skin diseases and degenerative neurological disorders [18,19]. Although there are reports suggesting that niacin can improve chromosomal/DNA damage in cryopreserved sperm, there is no direct research evidence exploring the relationship between niacin and niacinamide and male infertility. In a study on

the effect of niacinamide on oocytes, it was mentioned that supplementation of niacinamide promoted oocyte maturation and fertilization, while reducing oxidative stress in mouse oocytes[20]. This may provide a new perspective for understanding the mechanisms underlying NOA. Finally, alterations in pyruvate metabolism, a central energy-yielding pathway, likely disrupt the optimal energy supply essential for normal spermatogenesis [21].

In conclusion, our findings indicate that the pathogenesis of NOA involves coordinated dysregulations across multiple metabolic pathways, primarily related to energy metabolism and oxidative stress. This multi-faceted perspective provides a deeper theoretical foundation for understanding the metabolic mechanisms underlying NOA.

This study has several limitations. The seminal-plasma cohort was small and recruited at one center, the comparator group comprised normospermic men rather than men with obstructive azoospermia, and the ROC estimates were derived from the discovery cohort without external validation. The transcriptomic analysis used a separate public cohort and testicular tissue rather than matched seminal-plasma samples. These limitations restrict conclusions about clinical specificity, generalizability, and mechanism.

Conclusions

Integrated seminal-plasma metabolomics and public testicular transcriptomics identified altered purine, amino-acid, and energy-metabolism pathways in NOA. L-pipecolic acid, phenylpyruvic acid, and thymidine are candidate biomarkers, but this exploratory study does not establish clinical diagnostic utility. Larger independent cohorts, including men with obstructive azoospermia, are needed.

Declarations

Ethics approval and consent to participate

The study was approved by the Ethics Committee of the Second Hospital of Shanxi Medical University (approval no. 2023YX026). The requirement for informed consent was waived by the ethics committee.

Consent for publication

Not applicable. The manuscript contains no identifiable individual participant information.

Availability of data and materials

The public testicular transcriptomic dataset is available in the Gene Expression Omnibus under accession GSE4797. The seminal-plasma metabolomic data are not publicly deposited and are available from the corresponding authors on reasonable request.

Competing interests

The authors declare that they have no competing interests.

Funding

This study was funded by the Natural Science Foundation of Shanxi Province (202303021221203).

Authors' contributions

WW, PH, and JC conceptualized the study, performed the research and analysis, and drafted the manuscript. CL, YJ, and YX collected samples and organized data. SW and RT performed data analysis and visualization. YL and BH contributed to validation and manuscript review. YZ and QG verified results and refined the text. JW and CL supervised study design, coordinated the project, reviewed data, and finalized the manuscript. All authors read and approved the final manuscript.

Acknowledgements

Not applicable.

References

1. Badhai J, Schuster J, Gidlöf O, Dahl N. 5'UTR variants of ribosomal protein S19 transcript determine translational efficiency: implications for Diamond-Blackfan anemia and tissue variability. PLoS One 2011; 6(3): e17672.

2. McElreavey K, Jorgensen A, Eozenou C, Merel T, Bignon-Topalovic J, Tan DS, Houzelstein D, Buonocore F, Warr N, Kay RGG, Peycelon M, Siffroi JP, Mazen I, Achermann JC, Shcherbak Y, Leger J, Sallai A, Carel JC, Martinerie L, Le Ru R, Conway GS, Mignot B, Van Maldergem L, Bertalan R, Globa E, Brauner R, Jauch R, Nef S, Greenfield A, Bashamboo A. Pathogenic variants in the DEAH-box RNA helicase DHX37 are a frequent cause of 46,XY gonadal dysgenesis and 46,XY testicular regression syndrome. Genet Med 2020; 22(1): 150-159.

405 3. Xu Y, Lu H, Wang Y, Zhang Z, Wu Q. Comprehensive metabolic profiles of seminal plasma with different
406 forms of male infertility and their correlation with sperm parameters. J Pharm Biomed Anal 2020; 177: 112888.
407 4. Tremellen K. Oxidative stress and male infertility--a clinical perspective. Hum Reprod Update 2008; 14(3):
408 243-58.
409 5. Agarwal A, Sharma RK, Sharma R, Assidi M, Abuzenadah AM, Alshahrani S, Durairajanayagam D, Sabanegh
410 E. Characterizing semen parameters and their association with reactive oxygen species in infertile men. Reprod
411 Biol Endocrinol 2014; 12: 33.
412 6. Roychoudhury S, Sharma R, Sikka S, Agarwal A. Diagnostic application of total antioxidant capacity in
413 seminal plasma to assess oxidative stress in male factor infertility. J Assist Reprod Genet 2016; 33(5): 627-635.
414 7. Sharma RK, Pasqualotto FF, Nelson DR, Thomas AJ, Agarwal A. The reactive oxygen species-total
415 antioxidant capacity score is a new measure of oxidative stress to predict male infertility. Hum Reprod 1999;
416 14(11): 2801-7.
417 8. Agarwal A, Wang SM. Clinical Relevance of Oxidation-Reduction Potential in the Evaluation of Male
418 Infertility. Urology 2017; 104: 84-89.
419 9. Tang B, Shang X, Qi H, Li J, Ma B, An G, Zhang Q. Metabonomic analysis of fatty acids in seminal plasma
420 between healthy and asthenozoospermic men based on gas chromatography mass spectrometry. Andrologia
421 2017; 49(9): e12744.
422 10. Meek S, Sutherland L, Wei J, Sturmey R, Binas B, Clinton M, Burdon T. Hypoxanthine
423 phosphoribosyltransferase (HPRT)-deficiency is associated with impaired fertility in the female rat. Mol Reprod
424 Dev 2020; 87(9): 930-933.
425 11. Ronquist G, Stegmayr B, Niklasson F. Sperm motility and interactions among seminal uridine, xanthine,
426 urate, and ATPase in fertile and infertile men. Arch Androl 1985; 15(1): 21-7.

12. Rostampour F, Biglari M, Vaisi-Raygani A, Salimi S, Tavilani H. Adenosine deaminase activity in fertile and infertile men. Andrologia 2012; 44 Suppl 1: 586-9.

13. Safarinejad MR. Effect of pentoxifylline on semen parameters, reproductive hormones, and seminal plasma antioxidant capacity in men with idiopathic infertility: a randomized double-blind placebo-controlled study. Int Urol Nephrol 2011; 43(2): 315-28.

14. Agarwal A, Hamada A, Esteves SC. Insight into oxidative stress in varicocele-associated male infertility: part 1. Nat Rev Urol 2012; 9(12): 678-90.

15. Williams-Ashman HG, Hatch R, Harvey SE. Protein O-carboxylmethylation in relation to male gamete production and function. Adv Enzyme Regul 1985; 23: 389-416.

16. Baranizadeh K, Bahmanzadeh M, Tavilani H, Ghiasvand T, Amiri I, Yavangi M, Shafiee G. Evaluation of methylenetetrahydrofolate reductase and S-adenosyl-methionine level in male infertility: A case-control study. Int J Reprod Biomed 2022; 20(4): 299-306.

17. Sharma A, Madan N. Role of niacin in current clinical practice. Minerva Med 2019; 110(1): 79-83.

18. Fania L, Mazzanti C, Campione E, Candi E, Abeni D, Dellambra E. Role of Nicotinamide in Genomic Stability and Skin Cancer Chemoprevention. Int J Mol Sci 2019; 20(23): 5946.

19. Liu D, Pitta M, Jiang H, Lee JH, Zhang G, Chen X, Kawamoto EM, Mattson MP. Nicotinamide forestalls pathology and cognitive decline in Alzheimer mice: evidence for improved neuronal bioenergetics and autophagy procession. Neurobiol Aging 2013; 34(6): 1564-1580.

20. Guo Z, Yang J, Yang G, Feng T, Zhang X, Chen Y, Feng R, Qian Y. Effects of nicotinamide on follicular development and the quality of oocytes. Reprod Biol Endocrinol 2022; 20(1): 70.

21. Yi XD, Zhanf YN, Xiao S, Lei XC. [Role and regulatory mechanism of glycometabolism of Sertoli cells in spermatogenesis]. Zhonghua Nan Ke Xue 2019; 25(10): 923-927.

449 Table 2 Upregulated differential metabolites

compound name	Formula	VIP	P-VALUE	Log fold change
Indole	C8H7N	1.240978575	0.043318618	0.519316558
Acetylleucine	C8H15NO3	1.076203431	0.04681225	0.398207791
Nicotinic acid	C6H5NO2	1.536593801	0.024979381	2.066853633
Isonicotinic acid	C6H5NO2	1.536593763	0.02497936	2.066854001
N-Acetyl-L-tyrosine	C11H13NO4	1.221677654	0.027130184	0.65464065
Selenomethionine	C5H11NO2S e	1.57856879	0.006132273	0.764200568
N-Propionylglycine	C5H9NO3	1.520392248	0.001546792	0.012462947
L-Pipecolic acid	C6H11NO2	2.011935857	4.48645E-05	1.089411091
N-Acetylglycine	C4H7NO3	1.513690048	0.00032044	0.546550222
3-Nitrotyrosine	C9H10N2O5	1.993850825	0.001664763	0.925502495
L-Pyroglutamic acid	C5H7NO3	1.498713533	0.003093447	1.28969984
D-Mannosamine	C6H13NO5	1.49207773	0.029259302	1.398876531
5-Hydroxytryptophan	C11H12N2O 3	1.23796452	0.025637489	2.997903727
D-Glucosamine	C6H13NO5	1.341634272	0.048719125	1.171863175
Hydroxyproline	C5H9NO3	1.860562441	0.048335215	0.793341253
L-alpha-Aspartyl-L-phenylalanine	C13H16N2O 5	2.274114898	0.000807536	0.85458601
L-Dopa	C9H11NO4	1.644594958	0.019214604	1.59286016
gamma-Glutamylmethionine	C10H18N2O 5S	1.983429514	0.000165301	1.18598532
Glycylproline	C7H12N2O3	1.668085198	0.025315951	0.918368118
L-Asparagine	C4H8N2O3	1.958725813	0.023276723	0.855104859
N6-Acetyl-L-lysine	C8H16N2O3	2.105033767	0.04899933	1.40032399
gamma-L-Glutamyl-L-valine	C10H18N2O 5	2.225049454	0.002732829	1.838334896
gamma-Glutamylalanine	C8H14N2O5	1.168046993	0.018846534	1.006718144
L-Ornithine	C5H12N2O2	1.237033813	0.037824798	1.024741194
5-Hydroxylysine	C6H14N2O3	1.751219324	0.000804161	0.829384999
Acetoacetic acid	C4H6O3	1.801469588	0.001504811	0.534289988
2-Oxobutanoic acid	C4H6O3	1.899599591	0.001612475	0.554181746
Anthranilic acid	C7H7NO2	1.574147508	0.021204567	0.664449792
Citraconic acid	C5H6O4	1.321086141	0.026035037	1.350520314

3-(3-Hydroxyphenyl)propanoic acid	C9H10O3	1.246344889	0.043256645	0.547477984
2-Hydroxyisobutyric acid	C4H8O3	1.305146502	0.021683061	0.478664959
2-Hydroxybutyric acid	C4H8O3	1.519791211	0.002994501	0.537047023
Picolinic acid	C6H5NO2	1.481199949	0.022540318	1.872818219
Dodecanedioic acid	C12H22O4	1.610772836	0.024857863	0.601025937
4-Hydroxybenzoic acid	C7H6O3	1.252855062	0.026955902	0.59003033
D-(+)-Mannose	C6H12O6	1.69315915	0.000578696	0.612017506
D-(+)-Glucose	C6H12O6	1.193495733	0.019356959	0.571725153
D-Galactose	C6H12O6	1.202997919	0.018108853	0.576241424
Cellobiose	C12H22O11	2.073882108	0.002415049	0.815825265
Isomaltose	C12H22O11	1.053512117	0.006584975	1.032473849
2-Methylglutaric acid	C6H10O4	1.526901441	0.007571532	0.770230811
Adipic acid	C6H10O4	1.652797572	0.001874366	0.795341179

450 Table 3 Down-regulated differential metabolites

compound name	**Formula**	**VIP**	**P-VALUE**	Log fold change
Phenylpyruvic acid	C9H8O3	2.805532904	6.64186E-05	-3.368336532
2'-Deoxyadenosine	C10H13N5O3	2.242879005	0.003179688	-2.241351347
trans-Cinnamic acid	C9H8O2	2.035025142	0.003118261	-2.133818106
Propionyl-CoA	C24H40N7O17P3S	1.697693551	0.027493613	-2.104950768
L-Methionine sulfone	C5H11NO4S	2.478697008	0.000592992	-1.803405819
Thymidine	C10H14N2O5	2.469809324	0.000269543	-1.775044053
4-(Trimethylammonio)butanoate	C7H15NO2	1.324838995	0.026098763	-1.71662762
Thiamine pyrophosphate	C12H19N4O7P2S+	2.477302432	0.000887858	-1.57449337
Adenosine	C10H13N5O4	2.264425207	0.000274109	-1.369636819
2-Methylcitric acid	C7H10O7	1.538802594	0.01343021	-1.15183433
Acetylcholine	C7H16NO2+	2.028522962	0.001771295	-1.089156144
Inosine	C10H12N4O5	2.266142898	0.030603961	-0.91985733
Bilirubin	C33H36N4O6	1.916458936	0.017485839	-0.916755181

Nicotinamide	C6H6N2O	2.487479123	6.05699E-06	-0.840839448
S-Adenosylmethionine	C15H22N6O5S	1.976995376	0.002578716	-0.763405953
2'-Deoxyguanosine-5'-diphosphate	C10H15N5O10P2	2.042364588	0.000221418	-0.759376576
Adenosine-5'-diphosphate	C10H15N5O10P2	1.895657237	0.003392882	-0.724276607
Guanosine-5'-diphosphate	C10H15N5O11P2	2.07556471	0.000603567	-0.673168169
Hydroxyphenyllactic acid	C9H10O4	1.373257358	0.028422777	-0.630268659
L-Threonic acid	C4H8O5	1.702079361	0.022772909	-0.604436319
Glycolic Acid	C2H4O3	1.616816304	0.003933355	-0.601205639
2-Methylbenzoic acid	C8H8O2	2.09959986	0.000256447	-0.579911922
Flavin adenine dinucleotide	C27H33N9O15P2	1.209541373	0.042850875	-0.529612271
Propionylcarnitine	C10H19NO4	1.522845256	0.008560349	-0.514248925
Alloxan	C4H2N2O4	1.810062986	0.000974491	-0.496102404
Lactic acid	C3H6O3	1.21951983	0.043357819	-0.482212166
L-Carnitine	C7H15NO3	1.724275639	0.000480833	-0.442793558
O-Acetylcarnitine	C9H18NO4+	1.852478097	0.001822285	-0.397939878
alpha-Linolenic acid	C18H30O2	1.611781087	0.024932839	-0.342257921
Trimethoprim	C14H18N4O3	1.473691189	0.045570096	-0.018159771
N-Methylnicotinamide	C7H8N2O	1.673611056	0.021872301	-0.016312535

451